

## Short communication

Spark plasma sintered  $\beta$ -phase silicon nitride with Sr and Ca as a sintering aid for load bearing medical applicationsMaria Pettersson<sup>a,\*</sup>, Zohreh Pakdaman<sup>a</sup>, Håkan Engqvist<sup>a</sup>, Yi Liu<sup>b</sup>, Zhijian Shen<sup>b</sup>, Erik Östhols<sup>c</sup><sup>a</sup> Applied Material Science, Uppsala University, Ångström Laboratory, Lägerhyddsvägen 1, 75121 Uppsala, Sweden<sup>b</sup> Department of Materials and Environmental Chemistry, Stockholm University, Arrhenius Laboratory, 10691 Stockholm, Sweden<sup>c</sup> Sandvik Tooling, 126 80 Stockholm, Sweden

Available online 23 January 2012

## Abstract

Due to its inherent good physical and chemical properties silicon nitride has high potential to be used for load bearing implants. However, the standard sintering additives alumina and rare earth oxides are limiting the biocompatibility of the material. The aim of the current project is to exchange the additives for more biologically beneficial additives. Spark plasma sintered silicon nitride was manufactured with strontium or calcium as sintering aids. The ability of forming high strength  $\beta$ -phase microstructure silicon nitride was investigated. Powders were prepared with 10 and 30 wt.% glass phase and sintered at 1600, 1650, 1700 and 1750 °C. X-ray diffraction demonstrated compositions with 10 wt.% glass phase with strontium as sintering aid to yield larger amount of  $\beta$ -phase. The highest amount of  $\beta$ -phase (96% of the crystalline structure) was obtained using SPS for strontium-doped silicon nitride at sintering temperature 1750 °C, resulting in the highest fracture toughness, 4.2 MPa m<sup>1/2</sup>.  
© 2012 Elsevier Ltd. All rights reserved.

**Keywords:** Spark plasma sintering; Si<sub>3</sub>N<sub>4</sub>; Strontium; Calcium; Biomedical applications

## 1. Introduction

During the last decades silicon nitride (Si<sub>3</sub>N<sub>4</sub>) has been a subject of investigations for biomedical applications, especially for implants requiring high mechanical strength.<sup>1–3</sup> In load bearing applications such as hip and knee joints, the property profile that Si<sub>3</sub>N<sub>4</sub> can offer, i.e. high wear resistance, low friction, high fracture toughness, low density and non-toxic chemical composition, has a great potential compared to current implant materials. In particular  $\beta$ -phase Si<sub>3</sub>N<sub>4</sub> can obtain high fracture toughness, due to that it easily grows elongated grains, which can increase the material crack propagation resistance.<sup>4,5</sup> In addition to the mechanical properties, the chemical elements, silicon and nitrogen, are promising for use in biological applications.<sup>6,7</sup> Silicon nitride ceramics are today used as spinal implants, and recently a femoral head was implanted in a hip replacement.<sup>3,8</sup>

To obtain a dense Si<sub>3</sub>N<sub>4</sub>, sintering aids are used (to enable liquid phase sintering), since pure Si<sub>3</sub>N<sub>4</sub> dissociates before

complete densification.<sup>4,9</sup> Commonly, aluminum oxide and various rare earth or lanthanide oxides, such as yttrium oxide and magnesia, are used. In this study two combinations of sintering aids are investigated, Si<sub>3</sub>N<sub>4</sub> plus strontium (Sr) and Si<sub>3</sub>N<sub>4</sub> plus calcium (Ca). Both sintering aids are of interest for biomedical applications, Sr for its ability to increase bone formation, and decrease bone resorption<sup>10,11</sup> and Ca because it is the main element in hydroxyapatite and has successfully been used as a sintering aid for SiAlON previously.<sup>12–14</sup> A comparatively large amount of sintering aid was used, 10 and 30 wt.%, with the aim of acquiring some of the properties of bioglass, since bioglass has a high bone bioactivity.<sup>15</sup>

Spark plasma sintering (SPS) was used to densify the Si<sub>3</sub>N<sub>4</sub> based materials. An advantage with SPS, compared to for example hot pressing, is the short sintering times. Another advantage with SPS compared to conventional sintering methods, is that lower temperatures can be used for sintering, which, in combination with the short sintering times, allow for smaller grain sizes.<sup>16,17</sup>

During the sintering process, sintering aids react with added silica (SiO<sub>2</sub>) and creates an oxide melt. A transformation from  $\alpha$ - to  $\beta$ -Si<sub>3</sub>N<sub>4</sub> can take place, at high temperature  $\alpha$ -phase dissolves

\* Corresponding author.

E-mail address: [maria.pettersson@angstrom.uu.se](mailto:maria.pettersson@angstrom.uu.se) (M. Pettersson).

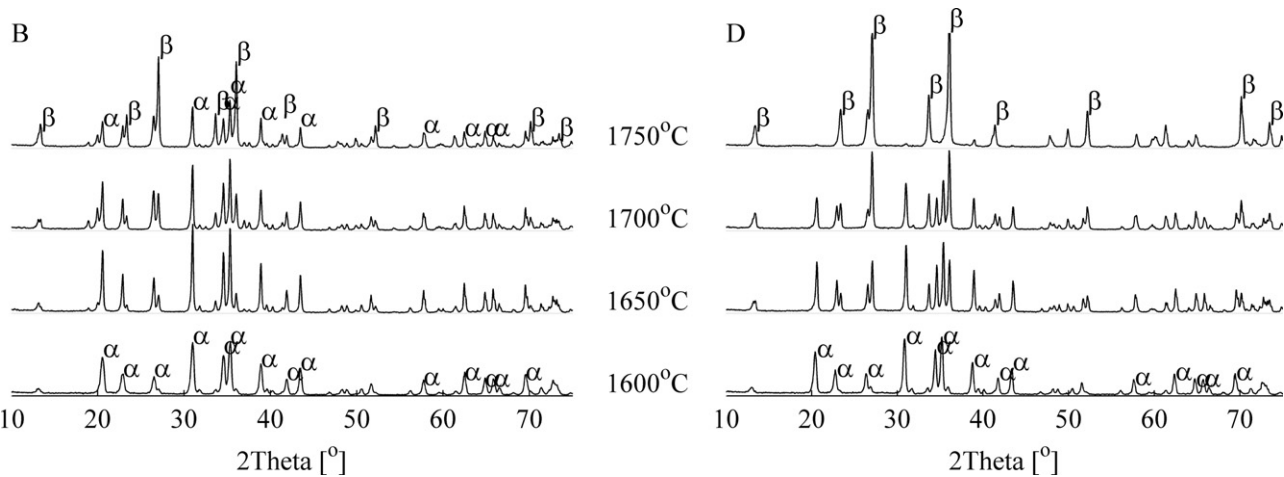


Fig. 1. XRD-spectra for sintered samples from powders B and D, at sintering temperatures 1600–1750 °C.

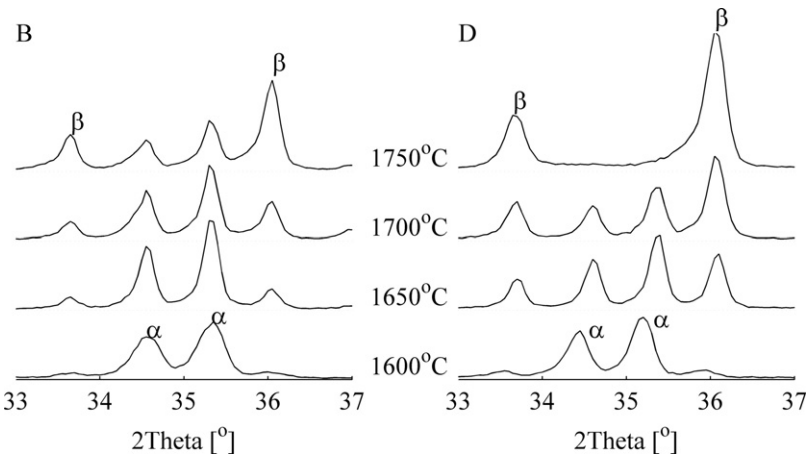
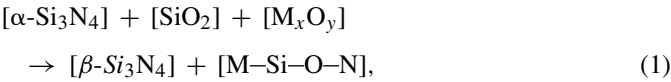


Fig. 2. XRD-spectra for sintered samples from powders B and D show more narrow spectra from Fig. 1. It demonstrates how the  $\alpha$ - and  $\beta$ -phase changes with increased sintering temperatures, from 1600 °C to 1750 °C.

in the liquid phase, and  $\beta$ -phase grains are precipitated according to



where M is the metal used as sintering aid, here Sr or Ca. Around the  $\beta$  grains the liquid phase solidifies into M–Si–O–N glass phase.<sup>18</sup>

The aim in this study is to form dense  $\beta$ -Si<sub>3</sub>N<sub>4</sub> with high fracture toughness using biologically resorbable sintering aids. In this short communication the microstructure and mechanical

properties are investigated. The biocompatibility and bioactivity are subject for further research.

2. Experimental

Powders were prepared and evaluated according to the following procedure. A slurry of  $\alpha$ -Si<sub>3</sub>N<sub>4</sub> (>95%, SN-E10, UBE America Inc., USA), dispersing agent (Dispex A40), SiO<sub>2</sub> (Quartz, Carl Roth GmbH + Co. KG, Germany), CaCO<sub>3</sub> (Merck KGaA, Germany) or SrO<sub>3</sub> (Merck KGaA, Germany) and de-ionized water were milled in a vibration mill, with Si<sub>3</sub>N<sub>4</sub> based milling media. After wet sieving, the slurries were freeze granulated. The slurry was sprayed into liquid nitrogen, and the

Table 1  
Powder composition and theoretical amount of glass phase.

Powder	$\alpha$ -Si <sub>3</sub> N <sub>4</sub> [wt. %]	SiO <sub>2</sub> [wt. %]	CaCO <sub>3</sub> [wt. %]	SrCO <sub>3</sub> [wt. %]	Glass phase [%]
A	69	26	5	0	30
B	89	9	2	0	10
C	65	21	0	14	30
D	89	7	0	4	10

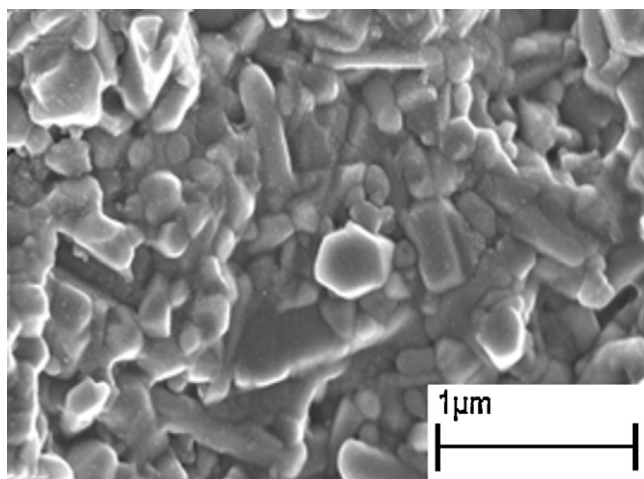


Fig. 3. SEM micrograph of the microstructure for sintered sample D, sintered at 1750 °C.

resulting powder was freeze dried for several days and then sieved through a 600 μm mesh.

The powder compositions are given in Table 1 with theoretical amounts of glass phase, assuming glass phase forms according to Eq. (1).

Powders (~5 g) were loaded in a graphite die, inner diameter 20 mm, and placed in the SPS instrument (Dr. Sinter 2050, SPS Syntex Inc., Japan). The sintering process started with a temperature increase from 600 to 650 °C during 3 min. Meanwhile the load on the sample was increased from 1.2 to 15.7 kN corresponding to pressures 3.8 and 50 MPa, respectively. That

pressure was kept constant during the rest of the process, while the sintering temperature was increased with 100 °C/min until a desired maximum temperature was reached. The sintering temperature was then held constant for 3 min. The maximum sintering temperatures used in this study were 1600, 1650, 1700 and 1750 °C.

Crystalline structures of the sintered samples were identified with X-ray diffraction (XRD, Diffraktometer D5000, Siemens and X'pert Pro, PANalytical) and quantification of β-phase according to the Rietveld method.<sup>19,20</sup> The microstructure was studied in a scanning electron microscope (SEM, Zeiss LEO 1550).

Sintered samples from the powders B and D (~10% glass phase), were investigated with respect to hardness (HV10), fracture toughness (interpreted from the crack length from the indentations) and density (Archimedes' principle).

### 3. Results and discussion

X-ray diffraction showed three crystalline phases in the sintered samples; α-Si<sub>3</sub>N<sub>4</sub>, β-Si<sub>3</sub>N<sub>4</sub> and Si<sub>2</sub>N<sub>2</sub>O.<sup>21–23</sup> Powders B and D change from α- to β-phase with increasing sintering temperature from 1600 up to 1750 °C, see Fig. 1. The progression is displayed for narrower angles in Fig. 2. Quantitative analysis enables estimation of the dominant crystalline phase. When a maximum sintering temperature of 1750 °C was used, powder B and C formed β-Si<sub>3</sub>N<sub>4</sub> as the predominant phase and powder A formed Si<sub>2</sub>N<sub>2</sub>O. Powder D sintered at 1700 and 1750 °C formed β-Si<sub>3</sub>N<sub>4</sub> as the predominant phase, at 1750 °C

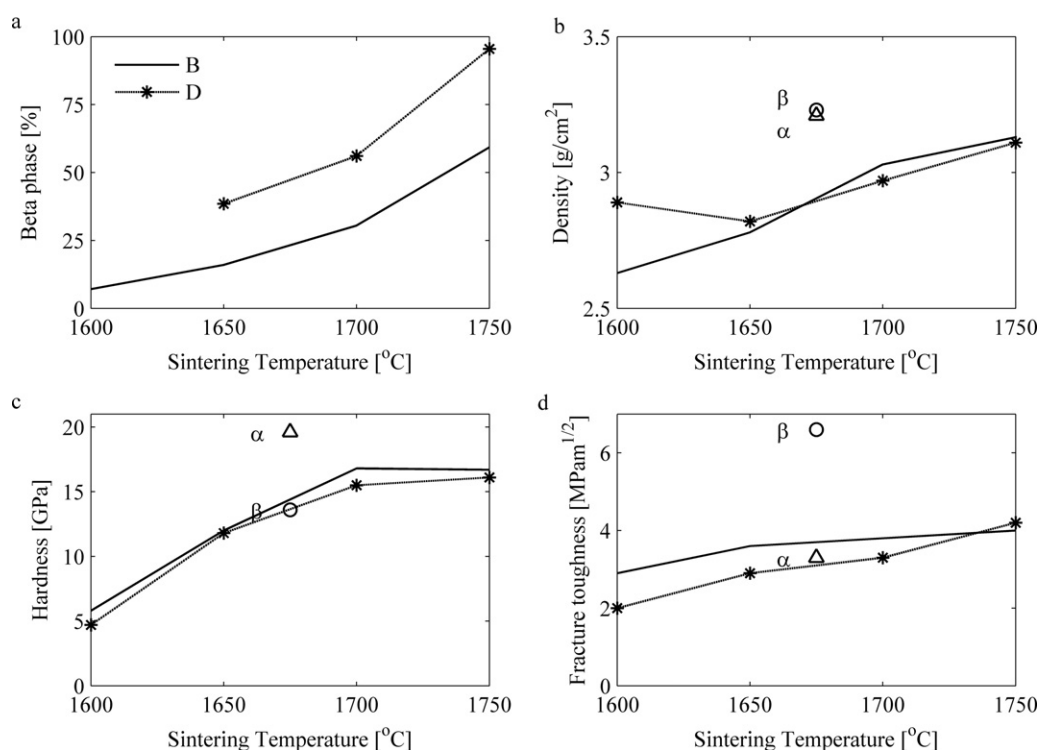


Fig. 4. Mechanical and chemical properties for powders B and D at sintering temperatures from 1600 °C to 1750 °C. Where (a) is the amount of β-Si<sub>3</sub>N<sub>4</sub> in the crystalline structures, (b) density, (c) Vickers hardness and (d) fracture toughness. Data for crystalline α and β-Si<sub>3</sub>N<sub>4</sub> from Gomes are given as a reference, sintered from 87 wt.% α-Si<sub>3</sub>N<sub>4</sub>.<sup>24</sup>

Table 2  
Dominant phase in sintered samples.

Powder	Sintering temperature [°C]			
	1600	1650	1700	1750
A	$\alpha$ -Si <sub>3</sub> N <sub>4</sub>	$\alpha$ -Si <sub>3</sub> N <sub>4</sub>	$\alpha$ -Si <sub>3</sub> N <sub>4</sub>	Si <sub>2</sub> N <sub>2</sub> O
B	$\alpha$ -Si <sub>3</sub> N <sub>4</sub>	$\alpha$ -Si <sub>3</sub> N <sub>4</sub>	$\alpha$ -Si <sub>3</sub> N <sub>4</sub>	$\beta$ -Si <sub>3</sub> N <sub>4</sub> (59%)
C	$\alpha$ -Si <sub>3</sub> N <sub>4</sub>	$\alpha$ -Si <sub>3</sub> N <sub>4</sub>	$\alpha$ -Si <sub>3</sub> N <sub>4</sub>	$\beta$ -Si <sub>3</sub> N <sub>4</sub> (68%)
D	$\alpha$ -Si <sub>3</sub> N <sub>4</sub>	$\alpha$ -Si <sub>3</sub> N <sub>4</sub>	$\beta$ -Si <sub>3</sub> N <sub>4</sub> (56%)	$\beta$ -Si <sub>3</sub> N <sub>4</sub> (96%)

approximately 96%  $\beta$ -phase was formed. The predominant phases for the different samples are summarized in Table 2.

The sintering aid Sr (C and D) results in higher amounts of  $\beta$ -phase compared to Ca. For the lower amounts of glass phase (10%, B and D) higher concentrations of  $\beta$ -phase are formed. The elongated  $\beta$ -phase grains are shown for sample D sintered at 1750 °C in Fig. 3.

Kitayama et al. have shown that for hot pressed Si<sub>3</sub>N<sub>4</sub>, with added rare earth oxides as sintering aids, the amount of  $\beta$ -phase increased with increasing sintering time.<sup>25</sup> Possibly an increased holding time could have the same effect for the samples in this study, and could be the subject of further work.

The mechanical properties of sample B and D (10% glass phase) were investigated, since they showed a higher ability to form  $\beta$ -Si<sub>3</sub>N<sub>4</sub>. The amount of  $\beta$ -Si<sub>3</sub>N<sub>4</sub>, density, hardness and fracture toughness are presented in Fig. 4. Hot pressed Si<sub>3</sub>N<sub>4</sub> with  $\alpha$ - and  $\beta$ -Si<sub>3</sub>N<sub>4</sub> phase are marked in the figure as a reference.

For B and D, an increased proportion of  $\beta$ -Si<sub>3</sub>N<sub>4</sub> formed at higher sintering temperatures. Sintered samples of powder D (with Sr as sintering aid) form more  $\beta$ -Si<sub>3</sub>N<sub>4</sub> (96%) than sintered samples of powder B, see Fig. 4a.

The density, hardness and fracture toughness also increased with increasing sintering temperature, see Fig. 4b–d.

Samples B and D have lower density, (2.6–3.1 g/cm<sup>3</sup>) than the reference. This is probably due to lighter amorphous phase and some porosity. The hardness increment with sintering temperature was most probably due to denser samples. The highest hardness obtained was 17 GPa.

The increase in fracture toughness with higher sintering temperatures could be due to increased grain size, but the grain size was not investigated in this study. A maximum fracture toughness of 4.2 MPa m<sup>1/2</sup> was reached. Other workers have under certain controlled conditions reached a fracture toughness of 10 MPa m<sup>1/2</sup>.<sup>5,26</sup> Compared with Gomes  $\alpha$ -Si<sub>3</sub>N<sub>4</sub>, the SPS produced samples have similar fracture toughness. To reach such high fracture toughness for the  $\beta$ -Si<sub>3</sub>N<sub>4</sub>, the grain size and amount of amorphous phase have to be optimized.

#### 4. Conclusions

This work has shown that dense  $\beta$ -Si<sub>3</sub>N<sub>4</sub> can be manufactured using SPS and only the bioresorbable substances Sr or Ca as sintering additives. The sintering process and powder composition need to be optimized further to reach the desired fracture toughness.

The highest amount of  $\beta$ -phase (approximately 96%) in the crystalline part of the sample was obtained at sintering temperature 1750 °C with Sr as sintering aid. A hardness of 17 GPa, a fracture toughness of 4.2 MPa m<sup>1/2</sup> and a density of 3.1 g/cm<sup>3</sup> were obtained. The results are promising for further evaluation of Si<sub>3</sub>N<sub>4</sub> for load bearing implants.

#### References

- Mazzocchi M, Bellosi A. On the possibility of silicon nitride as a ceramic for structural orthopaedic implants. Part I: processing, microstructure, mechanical properties, cytotoxicity. *J Mater Sci: Mater Med* 2008;**19**(8): 2881–7.
- Mazzocchi M, Gardini D, Traverso PL, Faga MG, Bellosi A. On the possibility of silicon nitride as a ceramic for structural orthopaedic implants. Part II: chemical stability and wear resistance in body environment. *J Mater Sci: Mater Med* 2008;**19**(8):2889–901.
- Sonny Bal B, Khandkar A, Lakshminarayanan R, Clarke I, Hoffman AA, Rahaman MN. Fabrication and testing of silicon nitride bearings in total hip arthroplasty. *J Arthroplasty* 2009;**24**(1):110–6.
- Riley FL. Silicon nitride and related materials. *J Am Ceram Soc* 2000;**83**(2):245–65.
- Becher PF, Sun ES, Plucknett KP, Alexander KB, Hsueh CH, Lin H-T, et al. Microstructural design of silicon nitride with improved fracture toughness: I, effect of grain shape and size. *J Am Ceram Soc* 1998;**81**(11): 2821–30.
- Guedes ESilva CC, König Jr B, Carbonari MJ, Yoshimoto M, Allegrini Jr S, Bressiani JC. Tissue response around silicon nitride implants in rabbits. *J Biomed Mater Res - Part A* 2008;**84**(2):337–43.
- Guedes e Silva CC, König Jr B, Carbonari MJ, Yoshimoto M, Allegrini Jr S, Bressiani JC. Bone growth around silicon nitride implants – an evaluation by scanning electron microscopy. *Mater Charact* 2008;**59**(9): 1339–41.
- Amedica Corporation Homepage, 2011-02-17. Retrieved 2011-11-15 from <http://amedica.com/company/news/02.17.11.pdf>.
- Richerson DW. *Modern ceramic engineering: properties, processing and use in design*. New York: Marcel Dekker, Inc.; 1992.
- Marie PJ, Ammann P, Boivin G, Rey C. Mechanisms of action and therapeutic potential of strontium in bone. *Calcif Tissue Int* 2001;**69**: 121–9.
- Grynias MD, Hamilton E, Cheng R, Tsouderos Y, Deloffre P, Hott M, et al. Strontium increased vertebral bone volume in rats at a low dose that does not induce detectable mineralization defect. *Bone* 1996;**18**(3):253–9.
- Wang PL, Zhang C, Sun WY, Yan DS. Characteristics of Ca- $\alpha$ -SiAlON-phase formation, microstructure and mechanical properties. *J Eur Ceram Soc* 1999;**19**:553–60.
- van RutenJWT, HintzenHT, Metselaar R. Phase formation of Ca- $\alpha$ -SiAlON by reaction sintering. *J Eur Ceram Soc* 1996;**16**:995–9.
- Hewett CL, Cheng Y-B, Muddle BC. Phase relationships and related microstructural observations in the Ca-Si-Al-O-N system. *J Am Ceram Soc* 1998;**81**(7):1781–8.
- Hench LL. Bioceramics: from concept to clinic. *J Am Ceram Soc* 1991;**74**(7):1487–510.
- Herrmann M, Shen Z, Schulz I, Hu J, Jancar B. Silicon nitride nanoceramics densified by dynamic grain sliding. *J Mater Res* 2010;**25**(12):2354–61.
- Nishimura T, Xu X, Kimoto K, Hirosaki N, Tanaka H. Fabrication of silicon nitride nanoceramics-powder preparation and sintering: a review. *Sci Technol Adv Mater* 2007;**8**(7–8):635–43.
- Hampshire S. Silicon nitride ceramics – review of structure, processing and properties. *JAMME* 2007;**24**:43–50.
- Rietveld HM. Line profiles of neutron powder-diffraction peaks for structure refinement. *Acta Crystallogr* 1967;**22**:151–2.
- Rietveld HM. A profile refinement method for nuclear and magnetic structures. *J Appl Cryst* 1969;**2**:65–71.
- International Centre for Diffraction Data. Reference files:  $\alpha$ -Si<sub>3</sub>N<sub>4</sub> PDF no. 41-0360.

22. International Centre for Diffraction Data. Reference files:  $\beta$ - $\text{Si}_3\text{N}_4$  PDF no. 33-1160.
23. International Centre for Diffraction Data. Reference files:  $\text{Si}_2\text{N}_2\text{O}$  PDF no. 47-1627.
24. Gomes JR, Oliveira FJ, Silva RF, Osendi MI, Miranzo P. Effect of  $\alpha$ -/ $\beta$   $\text{Si}_3\text{N}_4$ -phase ratio and microstructure an the tribological behaviour up to 700 °C. *Wear* 2000;**239**:59–68.
25. Kitayama M, Hirao K, Kanzaki S. Effect of rare earth oxide additives on the phase transformation rates of  $\text{Si}_3\text{N}_4$ . *J Am Ceram Soc* 2006;**89**: 2612–8.
26. Kleebe H-J, Pezzotti G, Ziegler G. Microstructure and fracture toughness of  $\text{Si}_3\text{N}_4$  ceramics: combined role of grain morphology and secondary phase chemistry. *J Am Ceram Soc* 1999;**82**(7):1857–67.